Operando High-Pressure NMR and IR Study of the Hydroformylation of 1-Hexene by 1,1′-Bis(Diarylphosphino)metallocene-Modified Rhodium(I) Catalysts

Claudio Bianchini,* Werner Oberhauser, and Annabella Orlandini

Istituto di Chimica dei Composti Organometallici (ICCOM-CNR), Area di Ricerca CNR di Firenze, via Madonna del Piano 10, 50019 Sesto Fiorentino, Italy

Carlo Giannelli and Piero Frediani

Dipartimento di Chimica Organica, Università degli Studi di Firenze, Polo Scientifico, via della Lastruccia 13, 50019 Sesto Fiorentino, Italy

Received March 31, 2005

Some rhodium(I) complexes of the general formula [Rh(P−P)(COD)]X were synthesized and characterized by multinuclear NMR spectroscopy (COD = cyclocta-1,5-diene; P−P = 1,1′-bis(diphenylphosphino)ferrocene, dppf, X = BPh_4, PF_6; P−P = 1,1′-bis(diphenylphosphino)ruthenocene, dppr, X = BPh_4; P−P = 1,1′-bis(diphenylphosphino)osmocene, dppo, X = BPh_4, PF_6; P−P = 1,1′-bis(diphenylphosphino)octamethylferrocene, dppomf, X = BAr'_4; P−P = (1,1′-bis(di(*o*-isopropylphenyl)phosphino)ferrocene, *o*-^{i}Pr-dppf, X = BAr'_4). These complexes were employed as catalyst precursors for the hydroformylation of 1-hexene in THF either in standard autoclaves or in high-pressure (HP) NMR tubes and IR cells. All catalysts exhibited good activity (TOFs ranging from 700 to 1000 mol aldehyde (mol cat)$^{-1}$ h^{-1}) and moderate regioselectivity in *n*-heptanal (67−74%). Irrespective of the rhodium precursor, the HP-NMR experiments under catalytic conditions showed the formation of kinetic dicarbonyl products at room temperature, which were independently prepared by reaction of the COD precursors with 1 bar CO in THF. Square-planar dicarbonyl complexes containing two *cis* carbonyl groups were obtained with the dppf and dppomf ligands, while the precursors with the dppr, dppo, and *o*-^{i}Pr-dppf ligands gave trigonal-bipyramidal dicarbonyl complexes with the equatorial positions occupied by two carbonyl groups and by the metallocene metal atom. The complexes $[Rh(CO)_2(dppf)]PF_6$ and $[Rh(CO)_2(dppo)]PF_6$ were isolated in the solid state and characterized by single-crystal X-ray analysis. On increasing gradually the temperature of the HP-NMR hydroformylation experiments, the dppf, dppr, and dppo dicarbonyl complexes disappeared. Formed in their place were neutral five-coordinate hydride(dicarbonyl) complexes $RhH(CO)_2(P-P)$ that exist in solution as two rapidly equilibrating geometric isomers. The reaction of the *o*-^{i}Pr-dppf precursor with syngas at 60 °C gave a trigonal-bipyramidal dicarbonyl complex with a dative Fe−Rh bond, while the dppomf complex decomposed to various CO-containing rhodium complexes. Unlike HP-NMR spectroscopy, HP-IR spectroscopy showed no kinetic product at any stage of the catalytic reactions. Also, HP-IR spectroscopy allowed us to distinguish the ee and ea geometric isomers of the hydride(dicarbonyl) resting states with dppf, dppr, and dppo. Irrespective of the temperature, *o*-^{i}Pr-dppf formed a stable dicarbonyl complex as a result of the catalytic reaction, while the dppomf dicarbonyl was unstable under hydroformylation conditions, converting into phosphine-free carbonyl Rh compounds.

Introduction

1,1′-Bis(phosphino)metallocenes are potentially chelating tri- and bidentate ligands with many applications in homogeneous reactions catalyzed by transition metal compounds.[1] The success of these ligands in catalysis is largely due to their unique flexibility that allows one to design molecular structures with different sandwiched metals and substituents either on the cyclopentadienyl ligands (Cp) or on the phosphorus atoms. Most of the research work in catalysis has been carried out with palladium(II) precursors of the prototypical ligand 1,1′-bis(diphenylphosphino)ferrocene (dppf): representative catalytic reactions include cross-coupling reactions,[2] Heck reaction,[3] carbonylation of chloroarenes,[4] aryl halide amination,[5] hydroamination of alkynes,[6] glioxylate-ene reaction with chiral controllers,[7] alternating copolymerization of CO and ethylene,[8] and methoxycarbonylation of alkenes.[9]

* To whom correspondence should be addressed.

(1) (a) Colacot, T. J. *Platinum Met. Rev.* **2001**, *45*, 22. (b) Gan, K.-S.; Hor, T. S. A. In *Ferrocenes: Homogeneous Catalysis, Organic Synthesis, Materials Science*; Togni, A., Hayashi, T., Eds.; VCH-Wiley: Weinheim, 1995; Chapter 1.

10.1021/om0502411 CCC: $30.25
Publication on Web 06/16/2005

Chart 1

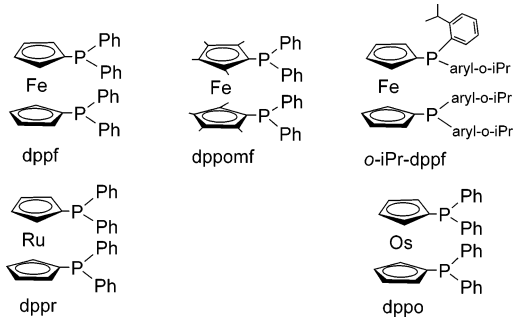

The hydroformylation of alkenes by 1,1′-bis(diarylphosphino)ferrocene rhodium(I) catalysts has been exclusively investigated by Unruh[10] and van Leeuwen.[11] Both authors have reported that the introduction of electron-withdrawing groups in the *para* position of the P-aryl rings increases the catalytic activity, while the regioselectivity is controlled by several factors, including the ligand basicity, the alkene, and the ligand-to-rhodium ratio.[10,11] Despite these excellent studies, much remains to understand on the structure−activity relationships regarding the hydroformylation of alkenes by 1,1′-bis-(diarylphosphino)metallocene rhodium catalysis. In particular, there is no information on hydroformylation catalysts containing a different metallocene metal than iron or bearing alkyl substituents either on the Cp's or in the *ortho* position of the P-aryl rings. Indeed, similar structural variations have been shown to affect remarkably both the activity and the selectivity of alkene alkoxycarbonylation reactions.[8a] The lack of such specific information on a reaction that still raises much interest both in industry and academically prompted us to study the hydroformylation of 1-hexene by a family of 1,1′-bis(diarylphosphino)metallocene rhodium(I) complexes where the chelating diphosphine ligand is dppf, dppo, dppr, dppomf, or isopropyl-dppf (Chart 1).

To acquire as much information as possible, standard methods, such as characterization of precursors and intermediates, reactions with isolated compounds, and batch catalytic reactions, have been backed up by *operando* high-pressure NMR and IR experiments.

Experimental Section

General Comments. All manipulations were routinely performed under an atmosphere of nitrogen, using Schlenk tubes. $[RhCl(COD)]_2$ and $NaBAr'_4$ ($Ar'_4 = m\text{-}(CF_3)_2C_6H_3$) were synthesized following reported procedures.[12,13] Likewise, the 1,1′-bis(diorganylphosphino)metallocene ligands were prepared as reported in the literature.[8c,14] 1-Hexene was purified by elution through a neutral Al_2O_3 (70−230 mesh) chromatographic column, followed by distillation and storage under nitrogen. Commercial *trans* hex-2-ene (purity > 99%) was used without further purification. Elemental analyses were performed with a Perkin-Elmer Series II CHNS/O analyzer. ^1H and $^{31}P\{^1H\}$ NMR spectra were recorded on a Varian VXR300 spectrometer operating at 299.94 and 121.42 MHz, respectively. $^{13}C\{^1H\}$ NMR spectra were recorded on a Varian Mercury 400 spectrometer operating at 100.57 MHz. High-pressure NMR experiments were performed on a Bruker ACP 200 spectrometer operating at 200.13 MHz for ^1H spectra and 81.01 MHz for $^{31}P\{^1H\}$ spectra. The 10 mm-o.d. sapphire tube was purchased from Saphikon, Milford, NH, while the titanium high-pressure charging head was constructed at ICCOM-CNR (Firenze, Italy).[15] *Caution*: *Since high gas pressures are involved, safety precautions must be taken at all stages of studies involving high-pressure NMR tubes.* IR spectra at atmospheric pressure as well as at high pressure were recorded with a FT-IR Perkin-Elmer BX spectrometer. The high-pressure IR cell, constructed at ICCOM-CNR, is constituted by a 75 mL autoclave equipped with ZnS windows (4 mm thickness, 8 mm diameter, optical path length 0.2 mm).[16] The hydroformylation reactions were performed in a 125 mL stainless steel autoclave, equipped with a magnetic drive stirrer and a Parr 4842 temperature and pressure controller. GC-MS analyses were carried out using a Shimadzu GCMS-QP5050A with a SP capillary column (length, 30 m; diameter, 0.25 mm; 0.1 μm film thickness). The hydroformylation products of 1-hexene were analyzed with a Shimadzu GC14 gas chromatograph coupled with a Shimadzu C-R4A computer equipped with a packed column (length, 2 m, diameter, 3.17 mm) of the type PPG LB-550-X 15% (polypropylene glycol (15%) supported on Chromosorb W) and a flame ionization detector. The residual amount of 1-hexene, the isomerization products of 1-hexene, and hexane were analyzed using a Perkin-Elmer 8320 gas chromatograph equipped with a capillary Chromopack column of Al_2O_3/Na_2SO_4 PLOT (length, 50 m; diameter, 0.45 mm) and a flame ionization detector.

Synthesis of [Rh(dppf)(COD)]X (X = BPh_4^-, 1a; PF_6^-, 1b). $[RhCl(COD)]_2$ (10 mg, 0.0203 mmol) was dissolved in 5 mL of methanol, solid dppf (22.50 mg, 0.0406 mmol) was added, and the resulting suspension was stirred for 1 h at room temperature to obtain a clear solution. A dark yellow crystalline precipitate of **1a** was obtained by adding $NaBPh_4$ (15.28 mg, 0.0447 mmol), which was filtered off, washed three times

(2) (a) Ogasawara, M.; Yoshida, K.; Hayashi, T. *Organometallics* **2000**, *19*, 1567. (b) Bosch, B. E.; Brümmer, I.; Kunz, K.; Erker, G.; Frölich, R.; Kotila, S. *Organometallics* **2000**, *19*, 1255. (c) Xie, Y.; Tan, G. K.; Yan, Y. K.; Vittal, J. J.; Ng, S. C.; Hor, T. S. A. *J. Chem. Soc., Dalton Trans.* **1999**, 773. (d) Fong, S.-W. A.; Hor, T. S. A. *J. Cluster Sci*. **1998**, *9*, 351. (e) Hayashi, T.; Konishi, M.; Kobori, Y.; Kumada, M.; Higuchi, T.; Hirotsu, K. *J. Am. Chem. Soc.* **1984**, *106*, 158.

(3) (a) Jutand, A.; Hii, K.-K. (Mimi); Thornton-Pett, M.; Brown, J. M. *Organometallics* **1999**, *18*, 5367. (b) Boyes, A. L.; Butler, I. R.; Quayle, S. C. *Tetrahedron Lett.* **1998**, *39*, 7763. (c) Brown, J. M.; Hii, K.-K. (Mimi) *Angew. Chem., Int. Ed*. **1996**, *35*, 657.

(4) Mägerlein, W.; Indolese, A. F.; Beller, M. *Angew. Chem., Int. Ed.* **2001**, *40*, 2856.

(5) (a) Hartwig, J. F. *Angew. Chem., Int. Ed.* **1998**, *37*, 2090. (b) Hartwig, J. F. *Acc. Chem. Res*. **1998**, *31*, 852. (c) Driver, M. S.; Hartwig, J. F. *J. Am. Chem. Soc.* 1996, *118*, 7217.

(6) (a) Li, K.; Horton, P. N.; Hursthouse, M. B.; Hii, K.-K. (Mimi) *J. Organomet. Chem*. **2003**, *665*, 250. (b) Müller, T. E.; Berger, M.; Grosche, M.; Herdtweck, E.; Schmidtchen, F. P. *Organometallics* **2001**, *20*, 4384.

(7) Mikami, K.; Aikawa, K. *Org. Lett.* **2002**, *4*, 99.

(8) (a) Bianchini, C.; Meli, A.; Oberhauser, W.; van Leeuwen, P. W. N. M.; Zuideveld, M. A.; Freixa, Z.; Kamer, P. C. J.; Spek, A. L.; Gusev, O. V.; Kal'sin, A. M. *Organometallics* **2003**, *22*, 2409. (b) Gusev, O. V.; Kal'sin, A. M.; Peterleitner, M. G.; Petrovskii, P. V.; Lyssenko, K. A.; Akhmedov, N. G.; Bianchini, C.; Meli, A.; Oberhauser, W. *Organometallics* **2002**, *21*, 3637. (c) Gusev, O. V.; Kalsin, A. M.; Petrovskii, P. V.; Lyssenko, K. A.; Oprunenko, Y. F.; Bianchini, C.; Meli, A.; Oberhauser, W. *Organometallics* **2003**, 22, 913.

(9) Bianchini, C.; Meli, A.; Oberhauser, W.; Parisel, S.; Gusev, O. V.; Kal'sin, A. M.; Vologdin, N. V.; Dolgushin, F. M. *J. Mol. Catal. A* **2004**, *224*, 35.

(10) Unruh, J. D.; Christenson J. R. *J. Mol. Catal*. **1982**, *14*, 19.

(11) Nettekoven, U.; Kamer, C. C. J.; Widhalm, M.; van Leeuwen, P. W. N. M. *Organometallics* **2000**, *19*, 4596.

(12) Giordano, G.; Crabtree, R. H. *Inorg. Synth.* **1979**, 218.

(13) Brookhart, M.; Grant, B.; Volpe, A. F. *Organometallics* **1992**, *11*, 3920.

(14) (a) Li, S.; Wei, B.; Low, P. M. N.; Lee, H. K.; Hor, T. S. A.; Xueb, F.; Mak, T. C. W. *J. Chem. Soc., Dalton Trans.* **1997**, 1289. (b) Hamann, B. C.; Hartwig, J. F. *J. Am. Chem. Soc.* **1998**, *120*, 3694 (c) Gusev, O. V.; Peterleitner, M. G.; Kal'sin, A. M.; Vologdin, N. V. *Russ. J. Electrochem.* **2003**, *39*, 1293. (d) Szymoniak, J.; Besanqon, J.; Dormond, A.; Moise, C. *J. Org. Chem.* **1990**, *55*, 1429. (e) Trouve, G.; Broussier, R.; Gautheron, B.; Kubicki, M. M. *Acta Crystallogr.* **1991**, *C47*, 1966.

(15) Bianchini, C.; Meli, A.; Traversi, A. Ital. Pat. FI A000025, 1997.

(16) Heaton, B. *Mechanisms in Homogeneous Catalysis, A Spectroscopic Approach*; Wiley-VCH: Weinheim, 2004.

with MeOH (2 mL), and then dried under vacuum. Yield: 41.39 mg (94%). Anal. Calcd for $C_{66}H_{60}BFeP_2Rh$: C, 73.08; H, 5.58. Found: C, 73.29; H, 5.75. Compound **1b** was synthesized by an identical procedure, using $NH_4(PF_6)$ (7.25 mg, 0.0445 mmol) instead of $NaBPh_4$. Yield: 33.27 mg (90%). Anal. Calcd for $C_{42}H_{40}FeF_6P_3Rh$: C, 55.43; H, 4.39. Found: C, 55.29; H, 4.20.

NMR data for **1a**: ^{1}H NMR (299.94 MHz, $CDCl_3$) δ 7.85−7.77 (m, 8H, P(C_6H_5)$_2$); 7.63−7.52 (m, 12H, P(C_6H_5)$_2$); 7.50−7.37 (m, 8H, *o*-B(C_6H_5)$_4$); 7.10−6.90 (m, 8H, *m*-B(C_6H_5)$_4$); 6.90−6.80 (m, 4H, *p*-B(C_6H_5)$_4$); 4.34 (m, 4H, C*H*(COD)); 4.29 (s, 4H, α-*H*(Cp)); 4.19 (s, 4H, *β*-*H*(Cp)); 2.26−2.04 (s, 8H, *CH*$_2$(COD)); ^{31}P{^{1}H} NMR (121.42 MHz, $CDCl_3$) δ 23.12 (d, ^1J(RhP) = 148.5 Hz).

NMR data for **1b**: ^{1}H NMR (299.94 MHz, $CDCl_3$) δ 7.83−7.75 (m, 8H, P(C_6H_5)$_2$); 7.60−7.51 (m, 12H, P(C_6H_5)$_2$); 4.33 (m, 4H, C*H*(COD)); 4.30 (s, 4H, α-*H*(*Cp*)); 4.20 (s, 4H, *β*-*H*(*Cp*)); 2.28−2.10 (s, 8H, *CH*$_2$(COD)); ^{31}P{^{1}H} NMR (121.42 MHz, $CDCl_3$) δ 23.22 (d, ^1J(RhP) = 148.0 Hz).

Synthesis of [Rh(dppr)(COD)]BPh$_4$ (2). [RhCl(COD)]$_2$ (10 mg, 0.0203 mmol) was dissolved in 5 mL of methanol, dppr (24.34 mg, 0.0406 mmol) was added, and the resulting mixture was stirred for 1 h at room temperature. The addition of $NaBPh_4$ (15.28 mg, 0.0447 mmol) caused the precipitation of a dark yellow precipitate, which was filtered off, washed several times with 2 mL portions of MeOH, and dried under vacuum. Yield: 43.40 mg (94%). Anal. Calcd for $C_{66}H_{60}BP_2RhRu$: C, 70.16; H, 5.35. Found: C, 69.80; H, 5.20.

^{1}H NMR (299.94 MHz, $CDCl_3$) δ 7.83−7.75 (m, 8H, P(C_6H_5)$_2$); 7.61−7.49 (m, 12H, P(C_6H_5)$_2$); 7.45−7.37 (m, 8H, *o*-B(C_6H_5)$_4$); 7.05−6.98 (m, 8H, *m*-B(C_6H_5)$_4$); 6.90−6.82 (m, 4H, *p*-B(C_6H_5)$_4$); 4.72 (s, 4H, α-*H*(Cp)); 4.51 (s, 4H, *β*-*H*(Cp)); 4.24 (m, 4H, C*H*(COD)); 2.37−1.96 (s, 8H, C*H*$_2$(COD)); ^{31}P{^{1}H} NMR (121.42 MHz, $CDCl_3$) δ 20.48 (d, ^1J(RhP) = 149.8 Hz).

Synthesis of [Rh(dppo)(COD)]X (X = BPh$_4^-$, 3a; PF$_6^-$, 3b). [RhCl(COD)]$_2$ (10 mg, 0.0203 mmol) was dissolved in 5 mL of methanol, solid dppo (27.96 mg, 0.0406 mmol) was added, and the resulting reaction mixture was stirred for 1 h at room temperature. The addition of $NaBPh_4$ (15.28 mg, 0.0447 mmol) caused the precipitation of a dark yellow precipitate of **3a**, which was filtered off, washed several times with 2 mL of methanol, and dried under vacuum. Yield: 44.89 mg (90%). Anal. Calcd for $C_{66}H_{60}BP_2RhOs$: C, 65.03; H, 4.96. Found: C, 64.80; H, 4.83. Compound **3b** was synthesized analogously, using $NH_4(PF_6)$ instead of $NaBPh_4$. Yield of **3b**: 38.60 mg (91%). Anal. Calcd for $C_{42}H_{40}F_6P_3OsRh$: C, 48.30; H, 3.83 Found: C, 48.20; H, 3.73.

NMR data for **3a**: ^{1}H NMR (299.94 MHz, $CDCl_3$) δ 8.02−7.96 (m, 8H, P(C_6H_5)$_2$); 7.78−7.56 (m, 12H, P(C_6H_5)$_2$); 7.46−7.34 (m, 8H, *o*-B(C_6H_5)$_4$); 7.25−7.18 (m, 8H, *m*-B(C_6H_5)$_4$); 7.08−6.03 (m, 4H, *p*-B(C_6H_5)$_4$); 5.16 (s, 4H, α-*H*(Cp)); 4.83 (s, 4H, *β*-*H*(Cp)); 4.43 (m, 4H, C*H*(COD)); 2.37−2.12 (s, 8H, C*H*$_2$(COD)); ^{31}P{^{1}H} NMR (121.42 MHz, $CDCl_3$) δ 24.15 (d, ^1J(RhP) = 149.7 Hz);

NMR data for **3b**: ^{1}H NMR (299.94 MHz, $CDCl_3$) δ 8.02−7.96 (m, 8H, P(C_6H_5)$_2$); 7.78−7.56 (m, 12H, P(C_6H_5)$_2$); 5.16 (s, 4H, α-*H*(Cp)); 4.83 (s, 4H, *β*-*H*(Cp)); 4.43 (m, 4H, C*H*(COD)); 2.37−2.12 (s, 8H, C*H*$_2$(COD)); ^{31}P{^{1}H} NMR (121.42 MHz, $CDCl_3$) δ 24.23 (d, ^1J(RhP) = 149.1 Hz).

Synthesis of [Rh(dppomf)(COD)]BAr′$_4$ (4). [RhCl(COD)]$_2$ (20 mg, 0.0406 mmol) was dissolved in 5 mL of degassed dichloromethane, solid dppomf (54.0 mg, 0.081 mmol) was added, and the solution was stirred for 1 h at room temperature. Solid NaBAr′$_4$ (71.75 mg, 0.081 mmol) was added, and stirring was continued for another hour. The NaCl precipitate was removed by filtration through Celite. The dark yellow solution was concentrated to dryness under vacuum to give analytically pure **4**. Yield: 104 mg (74%). Anal. Calcd for $C_{82}H_{68}BF_{24}FeP_2Rh$: C, 56.57; H, 3.94. Found: C, 56.33; H, 3.85.

^{1}H NMR (299.94 MHz, $CDCl_3$) δ 7.81−7.38 (m, 32H, P(C_6H_5)$_2$ + B(C_6H_3(*m*-CF_3)$_2$)$_4$); 4.56 (m, 4H, C*H*(COD)), 2.40−2.04 (m, 8H, C*H*$_2$(COD), 1.63 (s, 12H, α-(C*H*$_3$)Cp); 1.58 (s, 12H, *β*-(C*H*$_3$)*Cp*); ^{31}P{^{1}H} NMR (121.42 MHz, $CDCl_3$) δ 23.22 (d, ^1J(RhP) = 145.8 Hz).

Synthesis of [Rh(*o*-^{i}Pr-dppf)(COD)]BAr′$_4$ (5). [RhCl(COD)]$_2$ (14.13 mg, 0.0287 mmol) was dissolved in 5 mL of oxygen-free dichloromethane, solid *o*-^{i}Pr-dppf (41.37 mg, 0.0573 mmol) was added, and the solution was then stirred for 1 h at room temperature. NaBAr′$_4$ (50.79 mg, 0.0573 mmol) was added, and stirring was continued for 1 h. The NaCl precipitate was removed by filtration of the solution through Celite, and the resulting solution was concentrated to dryness under vacuum to give analytically pure **5**. Yield: 64.40 mg (62%). Anal. Calcd for $C_{86}H_{76}F_{24}FeP_2Rh$: C, 57.48; H, 4.26. Found: C, 57.23; H, 4.12.

^{1}H NMR (299.94 MHz, $CDCl_3$) δ 7.66−6.83 (m, 32H, P(C_6H_5)$_2$ + B(C_6H_3(*m*-CF_3)$_2$)$_4$); 4.33 (s, 4H, α-*H*(Cp)) 4.20 (m, 4H, C*H*(COD)), 4.07 (s, 4H, *β*-*H*(Cp)), 3.86 (m, 4H, C*H*(CH_3)$_2$), 1.48−1.81 (m, 8H, C*H*$_2$(COD), 1.29 (d, ^3J(HH) = 6.4 Hz, 6H, (CH)C*H*$_3$)$_2$); 0.91 (d, ^3J(HH) = 6.4 Hz, 6H, (CH)C*H*$_3$)$_2$); ^{31}P-{^{1}H} NMR (121.42 MHz, $CDCl_3$) δ 29.97 (d, ^1J(RhP) = 150.1 Hz).

Synthesis of [Rh(CO)$_2$(dppf)]PF$_6$ (6) and [Rh(CO)$_2$-(dppo)]PF$_6$ (8). Both these complexes were obtained through an identical procedure; therefore only one reaction is described here. In a Schlenk tube containing 5 mL of oxygen-free CH_2Cl_2 was dissolved **1b** (**3b**) (0.0333 mmol). Then CO was bubbled through the solution for 5 min. The orange-red solution of **6** (or the yellow solution of **8**) was concentrated to dryness under vacuum, and the solid was suspended in *n*-pentane and stirred at room temperature for 10 min. Analytically pure **6** (**8**) was filtered off and dried under a slight stream of nitrogen. Yield of **6**: 24.06 mg (85%). Anal. Calcd for $C_{36}H_{28}F_6FeO_2P_3Rh$: C, 50.38; H, 3.29. Found: C, 50.60; H, 3.60. Yield of **8**: 26.6 mg (80%). Anal. Calcd for $C_{36}H_{28}F_6O_2OsP_3Rh$: C, 43.57; H, 2.82. Found: C, 43.86; H, 2.95.

NMR and IR data for **6**: ^{1}H NMR (299.94 MHz, CD_2Cl_2) δ 7.80−7.40 (m, 20H, P(C_6H_5)$_2$); 4.59 (s, 4H, α-*H*(Cp)), 4.28 (s, 4H, *β*-*H*(Cp)); ^{13}C{^{1}H} NMR (100.57 MHz, CD_2Cl_2) δ 181.90 (br s, *C*O), 133.57−129.50 (P(C_6H_5), 76.51 (t, ^2J(CP) = 6.0 Hz, α-*C*(Cp)), 74.66 (t, ^3J(CP) = 4.0 Hz, *β*-*C*(Cp)), 71.20 (d, ^1J(PC) = 64 Hz, *ipso*-*C*(Cp)); ^{31}P{^{1}H} NMR (121.42 MHz, CD_2Cl_2) δ 24.97 (d, ^1J(RhP) = 127.3 Hz); IR (KBr) 2094 (s), 2048 (s) cm^{-1}; IR (THF) 2098 (s), 2053 (s) cm^{-1}.

NMR and IR data for **8**: ^{1}H NMR (299.94 MHz, CD_2Cl_2) δ 7.75−7.50 (m, 20H, P(C_6H_5)$_2$); 5.51 (t, ^4J(PH) = 1.7 Hz, 4H, *β*-*H*(Cp)), 4.33 (t, ^3J(PH) = 1.8 Hz, 4H, α-*H*(Cp)); ^{13}C{^{1}H} NMR (100.57 MHz, CD_2Cl_2) δ 189.00 (br, m, *C*O), 134.36−127.98 (m, P(C_6H_5)$_2$, 73.45 (s, *β*-*C*(Cp)), 68.09 (t, ^2J(CP) = 5.2 Hz, α-*C*(Cp)), 68.0 (d, ^1J(CP) = 64.9 Hz, *ipso*-*C*(Cp); ^{31}P{^{1}H} NMR (121.42 MHz, CD_2Cl_2) δ 5.17 (d, ^1J(RhP) = 90.1 Hz); IR (KBr) 2023 (s), 1971 (s) cm^{-1}; IR (THF) 2027 (s), 1982 (s) cm^{-1}.

In Situ Synthesis of [Rh(CO)$_2$(dppr)]BPh$_4$ (7), [Rh-(CO)$_2$(dppomf)]BAr′$_4$ (9), and [Rh(CO)$_2$(*o*-^{i}Pr-dppf)]BAr′$_4$ (10). In a Schlenk tube containing 0.9 mL of oxygen-free CD_2Cl_2 was dissolved **2**, **4**, or **5** (0.03 mmol). After the tube was cooled to 0 °C, CO was bubbled into the CD_2Cl_2 solution for 5 min. The resulting solution was transferred into a 5 mm NMR tube for product characterization. All our attempts to isolate **7**, **9**, or **10** in the solid state were unsuccessful due to their fast decomposition in the absence of a protective CO atmosphere.

NMR and IR data for **7**: ^{1}H NMR (299.94 MHz, CD_2Cl_2) δ 7.83−7.40 (m, 20H, P(C_6H_5)$_2$), 7.40−6.80 (m, 20H, B(C_6H_5)$_4$); 5.26 (s, 4H, *β*-*H*(Cp)), 4.06 (s, 4H, α-*H*(Cp)); ^{13}C{^{1}H} NMR (100.57 MHz, CD_2Cl_2) δ 188.00 (br, m, *C*O), 164.03 (q, ^1J(CB) = 49.2 Hz, *ipso*-*C*(B(C_6H_5)$_4$), 135.39−121.70 (P(C_6H_5)$_2$ + B(C_6H_5)$_4$), 79.66 (s, *β*-*C*(Cp)), 75.44 (t, ^2J(CP) = 5.3 Hz, α-*C*(Cp)), 68.0 (d, ^3J(CP) = 64.9 Hz, *ipso*-*C*(Cp); ^{31}P{^{1}H} NMR

(121.42 MHz, CD_2Cl_2) δ 11.31 (d, ^1J(RhP) = 90.3 Hz); IR (THF) 2040 (m), 1991 (s) cm^{-1}.

NMR and IR data for **9**: ^{1}H NMR (299.94 MHz, CD_2Cl_2) δ 7.90−7.40 (m, 32H, P(C_6H_5)$_2$ + BAr′$_4$); 1.63 (s, 12H, α-CH_3(Cp)), 1.37 (s, 12H, β-CH_3(Cp)); ^{13}C{^{1}H} NMR (100.57 MHz, CD_2Cl_2) δ 182.0 (br m, *C*O), 162.10 (m, *ipso*-*C*(B(Ar′)$_4$, 135.37, 132.28, 129.0 (P(C_6H_5)), 134.80 (s, *o*-*C*(Ar′)), 124.58 (q, ^1J(CF) = 272.4 Hz, *C*F$_3$), 117.46 (s, *p*-*C*(Ar′)), 86.74 (s, α-*C*(Cp)), 86.11 (s, β-*C*(Cp)), 72.24 (d, ^1J(PC) = 57.8 Hz, *ipso*-*C*(Cp)), 12.30 (s, α-(*C*H$_3$)Cp), 8.32 (s, β-(*C*H$_3$)Cp); ^{31}P{^{1}H} NMR (121.42 MHz, CD_2Cl_2) δ 30.53 (d, ^1J(RhP) = 132.1 Hz); IR (THF) 2094 (s), 2044 (s) cm^{-1}.

NMR and IR data for **10**: ^{1}H NMR (299.94 MHz, CD_2Cl_2) δ 8.10−7.40 (m, 32H, P(C_6H_5)$_2$ + BAr′$_4$); 5.26 (br s, 4H, β-*H*(Cp)), 4.04 (br s, 4H, α-*H*(Cp)), 3.38 (m, 4H, C*H*(CH$_3$)$_2$), 0.88 (br s, 24H, (CH)C*H*$_3$)$_2$); ^{13}C{^{1}H} NMR (100.57 MHz, CD_2Cl_2) δ 190.20 (br m, *C*O), 162.20 (m, *ipso*-*C*(B(Ar′)$_4$, 153.09 (s, *C*(CH(CH$_3$)$_2$)), 134.80 (s, *o*-*C*(Ar′)), 133.27, 128.36, 126.83 (P(C_6H_5)), 124.58 (q, ^1J(CF) = 272.4 Hz, *C*F$_3$), 117.46 (s, *p*-*C*(Ar′)), 77.82 (br s, β-*C*(Cp)), 72.56 (br s, α-*C*(Cp)) + *ipso*-*C*(Cp), 32.49 (s, *C*H-(CH$_3$)$_2$), 22.92 (s, CH(*C*H$_3$)$_2$), 22.57 (s, CH(*C*H$_3$)$_2$); ^{31}P{^{1}H} NMR (121.42 MHz, CD_2Cl_2) δ 7.14 (d, ^1J(RhP) = 89.1 Hz); IR (THF) 2025 (m), 1980 (s) cm^{-1}.

In Situ Synthesis of RhH(CO)$_2$(dppf) (11), RhH(CO)$_2$-(dppr) (12), and RhH(CO)$_2$(dppo) (13). Compound **1b**, **2**, or **3b** (0.018 mmol) was dissolved in 1.8 mL of degassed THF-d_8, and the solution was transferred under nitrogen into a 10 mm-o.d. sapphire tube. The tube was pressurized with syngas (CO/H_2, 1:2) to a total pressure of 45 bar and then introduced into the NMR probe at room temperature. ^{31}P{^{1}H} NMR spectra acquired at different temperatures in the interval from 20 to 60 °C showed **1b** and **2** to convert completely into **11** and **12**, respectively, within 1 h, while **3b** converted into **13** only after heating at 60 °C for 3 h. NMR data for **11**,[11] **12**, and **13** are given at room temperature. Our attempts to isolate **11**, **12**, and **13** in the solid state were unsuccessful due to their instability in the absence of CO and H_2. The IR absorption spectra for **11**, **12**, and **13** were acquired at room temperature using a high-pressure IR cell pressurized at 45 bar of CO/H_2 (1:2).

NMR and IR data for **11**: ^{1}H NMR (200.13 MHz, TDF) δ 8.11−7.20 (m, 20H, P(C_6H_5)$_2$), 4.43 (s, 4H, α-*H*(Cp)), 4.16 (s, 4H, β-*H*(Cp)), −9.45 (td, ^1J(RhH) = 9.8 Hz, ^2J(PH) = 42.9 Hz, 1H, Rh-*H*); ^{31}P{^{1}H} NMR (81.01 MHz, TDF) δ 31.10 (d, ^1J(RhP) = 121 Hz); IR (THF): 2036 (w, ee), 1989 (m, ee and ea), 1945 (s, ea) cm^{-1} (ee: bis-equatorial coordination mode, ea: equatorial−axial coordination mode).

NMR and IR data for **12**: ^{1}H NMR (200.13 MHz, TDF) δ 8.11−7.20 (m, 20H, P(C_6H_5)$_2$), 4.52 (s, 4H, α-*H*(Cp)), 4.26 (s, 4H, β-*H*(Cp)), −9.60 (td, ^1J(RhH) = 7.8 Hz, ^2J(PH) = 30 Hz, 1H, Rh-*H*); ^{31}P{^{1}H} NMR (81.01 MHz, TDF) δ 30.5 (d, ^1J(RhP) = 128 Hz); IR (THF) 2038 (w, ee), 1990 (s, ee and ea), 1943 (s, ea) cm^{-1}.

NMR and IR data for **13**: ^{1}H NMR (200.13 MHz, TDF) (phenyl-*H* difficult to assign, overlapped with BAr′$_4$-H), δ 5.10 (s, 4H, α-*H*(Cp)), 4.90 (s, 4H, β-*H*(Cp)), −9.72 (td, ^1J(RhH) = 8.7 Hz, ^2J(PH) = 28.2 Hz, 1H, Rh-*H*); ^{31}P{^{1}H} NMR (81.01 MHz, TDF) δ 35.20 (d, ^1J(RhP) = 128.2 Hz); IR (THF) 2036 (w, ee), 1992 (m, ee and ea), 1942 (s, ea) cm^{-1}.

In Situ Reaction of 6 with Syngas in THF-d_8 and in CD_2Cl_2. A 10 mm-o.d. sapphire tube was charged first with 10.7 mg (0.0125 mmol) of compound **6** and dissolved in 1.8 mL of degassed TDF and then with 15 bar of CO. Afterward it was placed into the NMR probe at room temperature, and ^{31}P{^{1}H} NMR and ^{1}H NMR spectra were recorded. Only compound **6** was observed by ^{31}P{^{1}H} NMR spectroscopy. The NMR tube was removed from the probe and pressurized with 30 bar of hydrogen. Immediately after, ^{31}P{^{1}H} NMR and ^{1}H NMR spectra at room temperature were acquired. The conversion of **6** into the as yet unidentified compound **15** started, and after 1 h at room temperature nearly equal concentrations of **6** and **15** could be detected. Heating the TDF solution to higher temperature until 70 °C for 1 h gave the conversion of **15** into the known compound **11**. As compound **15** was unstable in the absence of syngas, only the significant chemical shifts are reported for this compound. An analogous HP-NMR experiment in CD_2Cl_2 exhibited only compound **6**. Neither **15** nor **11** was observed, even after prolonged heating at 70 °C. An analogous HP-IR experiment in THF as well as in CH_2Cl_2 gave no hint for the formation of **15**, as in THF only **11** was observed pressurizing the THF solution of **6** with CO/H_2 (15/30 bar) at room temperature, while in CH_2Cl_2 only compound **6** was observed, even at 70 °C. Due to the overlapping of the ^{1}H NMR signals in the phenyl region of compounds **6**, **11**, and **15**, no reliable phenyl signals for **15** can be reported.

NMR data for **15**: ^{1}H NMR (200.13 MHz, TDF) δ 5.10 (br s, β-*H*(Cp)), 4.25 (br s, α-*H*(Cp)); ^{31}P{^{1}H} NMR (81.01 MHz, TDF) δ 24.72 (d, ^1J(RhP) = 91.6 Hz).

Synthesis of RhH(CO)$_2$(dppomf) (14). Compound **4** (20 mg, 0.011 mmol) and NEt_3 (3.2 μL, 0.021 mmol) were dissolved in 1.8 mL of degassed THF-d_8. This mixture was transferred under nitrogen into a 10 mm-o.d. sapphire tube. The tube was pressurized with CO/H_2 (1:2) up to a total pressure of 45 bar and then introduced into the NMR probe at room temperature. The conversion of **4** into **14** was followed by ^{31}P{^{1}H} and ^{1}H NMR at room temperature. The conversion was complete after 15 min. The IR spectrum of **14** was acquired at room temperature after pressurizing the IR cell, containing a solution of **4** (20 mg, 0.011 mmol) and 3.2 μL (0.021 mmol) of NEt_3 in 24 mL of THF, up to 45 bar of CO/H_2 (1:2).

^{1}H NMR (200.13 MHz, TDF) δ 1.77 (s, 12H, α-CH_3(Cp)), 1.47 (s, 12H, β-CH_3(Cp)), −10.09 (td, ^1J(RhH) = 9.6 Hz, ^2J(PH) = 42.9 Hz, 1H, Rh-*H*); ^{31}P{^{1}H} NMR (81.01 MHz, TDF) δ 30.02 (d, ^1J(RhP) = 125.0 Hz); IR (THF) 2063 (w, ee), 1984 (m, ee and ea), 1941 (s, ea) cm^{-1}.

Batch Hydroformylation Reactions. Typically, a THF solution (25 mL) containing 2 μmol of the precatalyst and 2 mmol of 1-hexene was introduced by suction into the autoclave, previously evacuated by a vacuum pump. The autoclave was then pressurized at room temperature with CO and H_2 in a 1:2 ratio to a total pressure of 45 bar, stirred at 300 rpm, and then heated to the desired temperature. After the desired reaction time, the autoclave was cooled to room temperature and the gases were vented. The composition of the solution was analyzed by GC and GC-MS.

High-Pressure NMR Study in THF-d_8 of 1a, 2, 3a, 4, and 5 under Syngas Either in the Presence or Absence of 1-Hexene. All high-pressure NMR experiments were performed analogously; therefore only a typical procedure is described here. A 10 mm-o.d. sapphire tube was charged under nitrogen with 1.8 mL of a degassed THF-d_8 solution of each rhodium complex (0.0125 mmol). Then 1-hexene (156 μL, 1.25 mmol) was syringed into the NMR tube. ^{31}P{^{1}H} and ^{1}H NMR spectra were acquired at room temperature (20 °C). Afterward, the sapphire tube was removed from the NMR probe and charged with CO/H_2 (1:2) to a total pressure of 45 bar. The sapphire tube was placed again into the NMR probe and ^{31}P{^{1}H} NMR and ^{1}H NMR spectra were recorded every 10 °C from room temperature to 60 °C. After heating the solution for 1 h at 60 °C, the NMR probe was cooled to room temperature and ^{31}P{^{1}H} and ^{1}H NMR spectra were recorded.

Analogous experiments were carried out in the absence of 1-hexene, and no substantial difference was noticed in the ^{31}P{^{1}H} and ^{1}H NMR spectra.

High-Pressure IR Study in THF of 1a, 2, 3a, 4, and 5 under Syngas Either in the Presence or Absence of 1-Hexene. All high-pressure IR measurements were performed analogously; therefore only a typical procedure is described here. Compound **1a**, **2**, **3a**, **4**, or **5** (0.0315 mmol) was dissolved in 24 mL of oxygen-free THF. Then 1-hexene (390 μL, 3.15 mmol) was added, and the solution introduced into the high-pressure IR cell under nitrogen. The IR cell was

Table 1. Experimental X-ray Diffraction Parameters and Crystal Data of 6 and 8

	6	**8**
empirical formula	$C_{36}H_{28}F_6FeO_2P_3Rh$	$C_{36}H_{28}F_6O_2OsP_3Rh$
fw	858.25	992.60
cryst size (mm)	0.40 × 0.35 × 0.22	0.35 × 0.10 × 0.05
cryst syst	monoclinic	triclinic
space group	$P2_1/a$	$P\bar{1}$
a (Å)	9.662(2)	15.524(1)
b (Å)	36.711(10)	11.609(2)
c (Å)	9.971(2)	9.860(6)
α (deg)	90	87.74(3)
β (deg)	92.13(2)	81.50(2)
γ (deg)	90	93.50(1)
V (Å^3)	3534.2(1)	1752.1(1)
D_{calcd} (Mg/m^3)	1.613	1.881
Z	4	2
μ(Mo Kα) (mm^{-1})	1.077	4.295
F(000)	1720	960
diffractometer radiation	Enraf Nonius CAD4, λ(Mo Kα) = 0.71073 Å	
temp (K)	293(2)	293(2)
θ range for data collection (deg)	2.04−24.97	2.64−20.02
index range	$-11 \le h \le 11$	$-14 \le h \le 14$
	$0 \le k \le 43$	$-11 \le k \le 11$
	$0 \le l \le 11$	$0 \le l \le 9$
no. of reflns collected	6787	3597
no. of indep reflns	6192	3261
no. of refined params	442	322
R1 ($2\sigma(I)$)	0.0420	0.0673
R1 (all data)	0.0655	0.0993
wR2 (all data)	0.1086	0.1574
goodness of fit on F^2	0.963	1.006
largest diff peak and hole (e/Å^3)	0.727/−0.577	0.944/−0.968

pressurized at room temperature with CO/H_2 (1:2) to a total pressure of 45 bar and then placed into the spectrometer. Spectra were acquired at room temperature and at 60 °C under stirring. After 1 h at 60 °C, the spectra showed no significant change in the 4000−750 cm^{-1} region. Afterward the autoclave was cooled to room temperature and the gases were vented out. The GC-MS analysis of the solution showed the presence of COD and the formation of aldehydes with the same regioselectivity observed in the corresponding batch reactions.

Analogous HP-IR experiments, carried out without added 1-hexene, gave identical results.

X-ray Structure Determination. Single crystals of **6** and **8** were obtained by diffusion of *n*-hexane in a CH_2Cl_2 solution of **6** and **8** at room temperature. Diffraction data of **6** and **8** were collected at room temperature on an Enraf Nonius CAD4 automatic diffractometer with Mo Kα radiation (graphite monochromator). Unit cell parameters of both structures were determined from a least-squares refinement of the setting angles of 25 carefully centered reflections. Crystal data and data collection details are given in Table 1. The intensities were rescaled, and a standard deviation $\sigma(I)$ was calculated using the value of 0.03 for the instability factor k.[17] Lorentz−polarization and absorption corrections were applied.[18] Atomic scattering factors were taken from ref 19a, and an anomalous dispersion correction, real and imaginary part, was applied.[19b] The structures were solved by direct methods and refined by full-matrix F^2 refinement. Whereas in **6** anisotropic thermal parameters were assigned to all non-hydrogen atoms, in **8** the phenyl carbon atoms were refined isotropically, owing to the less favorable reflections to parameters *ratio*. Moreover in **8** the significant decay of the crystal has to be pointed out, which is responsible for the somewhat poor data. In both structures hydrogen atoms were introduced in their calculated positions, with thermal parameters 20% larger than those of the respective carbon atoms. The function minimized during the refinement was $\sum w(F_o^2 - F_c^2)^2$, where w is respectively defined as $1/[\sigma^2(F_o^2) + (0.0580P)^2 + 3.02P]$ (**6**) and $1/[\sigma^2(F_o^2) + (0.0218P)^2 + 82.41P]$ (**8**), where $P = (\max(F_o^2) + 2F_c^2)/3$. All the calculations were performed on a PC using the WINGX package[20a] with SIR-97,[20b] SHELX-97,[20c] and ORTEP-3 programs.[20d] Crystallographic data for the structures (excluding structure factors) reported in this paper have been deposited at the Cambridge Crystallographic Data Center: CCDC-266231 for **6**, CCDC-266232 for **8**. Copies of the data can be obtained free of charge on application to The Director, CCDC, 12 Union Road, Cambridge, CB21EZ, U.K. (fax, internat. +(1223) 336-033; e-mail, deposit@ccdc.cam.ac.uk; web, //www.ccdc.cam.ac.uk.

Chart 2

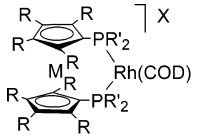

R': C_6H_5, M: Fe, R: H, X: BPh_4^- (**1a**); PF_6^- (**1b**)
R': C_6H_5, M: Ru, R: H, X: BPh_4^- (**2**)
R': C_6H_5, M: Os, R: H, X: BPh_4^- (**3a**); PF_6^- (**3b**)
R': C_6H_5, M: Fe, R: CH_3, X: BAr'_4^- (**4**)
R': $C_6H_4(C_3H_7)_2$, M: Fe, R: H, X:BAr'_4^- (**5**)

Results and Discussion

Synthesis and Characterization of the Rhodium Complexes Investigated in this Study. The COD catalyst precursors **1a,b**, **2**, **3a**,**b**, **4**, and **5** (Chart 2) were synthesized through two slightly different protocols. In the first procedure, a stoichiometric amount of the desired 1,1′-bis(diarlphosphino)metallocene ligand was added to a MeOH solution of $[RhCl(COD)]_2$. The further addition of $NaBPh_4$ or $NH_4(PF_6)$ allowed the isolation of the complex cation $[Rh(P-P)(COD)]^+$ as BPh_4^- or PF_6^- salt. This procedure could be applied only to the dppf, dppr, and dppo derivatives, as these diphosphine ligands show a low solubility in MeOH. In the case of dppomf and *o*-^{i}Pr-dppf, which are insoluble in methanol, both $[RhCl(COD)]_2$ and the diphosphine ligand were dissolved in dichloromethane, and the precipitation of the cationic metal complexes was achieved by adding $NaBAr'_4$. Unambiguous characterization of the [Rh(P−P)(COD)]X products was obtained by multinuclear NMR spectroscopy, IR spectroscopy, and elemental analysis. It is worth mentioning that all complexes exhibit a Rh−P coupling constant of ca. 150 Hz, which is typical for square-planar rhodium diphosphine complexes with a P−Rh−P bite angle close to 90°.[21]

(17) Corfield, P. W. R.; Doedens, R. J.; Ibers, J. A. *Inorg. Chem*. **1967**, *6*, 197.

(18) Parkin, S.; Moezzi, B.; Hope, H. *J. Appl. Crystallogr*. **1995**, *28*, 53.

(19) (a) Wilson, J. C. In *International Tables for X-ray Crystallography*; Kluwer: Dordrecht, 1992; p 500. (b) Wilson, J. C. In *International Tables for X-ray Crystallography*; Kluwer: Dordrecht, 1992; p 219.

(20) (a) Farrugia, L. J. *J. Appl. Crystallogr*. **1999**, 32, 837. (b) Altomare, A.; Burla, M. C.; Camalli, M.; Cascarano, G. L.; Giacovazzo, C.; Guagliardi, A.; Moliterni, G. G.; Polidori, G.; Spagna, R. *J. Appl. Crystallogr*. **1999**, *32*, 115. (c) Sheldrick, G. M. *SHELX-97*; University of Göttingen: Göttingen, Germany, 1997. (d) Burnett, M. N.; Johnson, C. K. *ORTEP-3*; Report ORNL-6895; Oak Ridge National Laboratory: Oak Ridge, TN, 1996.

(21) (a) Anderson, M. P.; Pignolet, L. H. *Inorg. Chem*. **1981**, *20*, 4101. (b) Bakos,. J.; Tóth, I.; Heil, B.; Szalontai, G.; Pàrkànyi, L.; Fülöp, V. *J. Organomet. Chem*. **1989**, *370*, 263. (c) Kalck, P.; Randrianalimanana, C.; Ridmy, M.; Thorez, A. *New J. Chem*. **1988**, *12*, 679.

Scheme 1

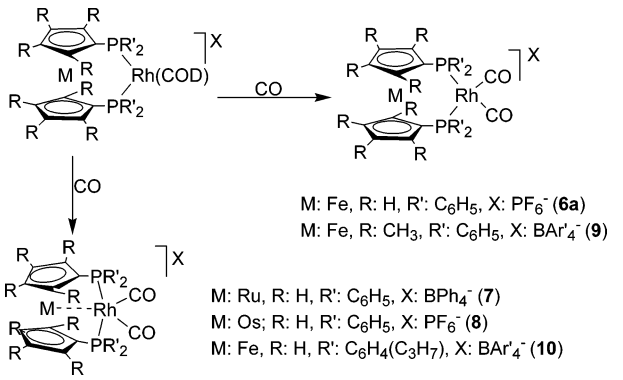

Since the HP-NMR experiments at room temperature showed the formation of dicarbonyl rhodium(I) complexes at the early stage of the hydroformylation reactions (vide infra), **1a**, **2**, **3b**, **4**, and **5** were independently reacted with CO in CH_2Cl_2 to see whether the dicarbonyl complexes could be isolated for authentication. Irrespective of the CO pressure (1−15 bar), monocationic dicarbonyl complexes of the formula $[Rh(CO)_2(P-P)]^+$ were selectively obtained (Scheme 1).

However, only two of them, namely, $[Rh(CO)_2(dppf)]PF_6$ (**6**) and $[Rh(CO)_2(dppo)]PF_6$ (**8**), could be isolated, while $[Rh(CO)_2(dppr)]PF_6$ (**7**), $[Rh(CO)_2(dppomf)]PF_6$ (**9**), and $[Rh(CO)_2(o\text{-}^i\text{Pr-dppf})]PF_6$ (**10**) were stable only in the presence of a protective CO atmosphere. The characterization of the latter complexes was therefore achieved by in situ HP-NMR and HP-IR techniques.

The dicarbonyl complexes exhibit two different coordination geometries: the dppf complex **6** and the dppomf complex **9** are square planar with *cis* CO ligands, while the dppr, dppo, and *o*-^{i}Pr-dppf complexes **7**, **8**, and **10** exhibit a distorted trigonal-bipyramidal coordination geometry due to an actual weak bonding interaction between the sandwiched metal and rhodium (Scheme 1). Distinctive features for a square-planar coordination about the rhodium center in **6** and **9** are a $^{31}P\{^1H\}$ NMR Rh−P coupling constant of 127 and 132 Hz, respectively, and two strong IR absorption bands, in THF solution, of almost equal intensity at 2098 and 2053 cm^{-1} for **6** and 2094 and 2044 cm^{-1} for **9**.[22] Moreover, small $\Delta\delta$ values separate the Cp α and β hydrogen atoms in **6** (0.42 ppm) as well as the Cp methyl groups in **9** (0.26 ppm), which indicates the absence of an intramolecular metal−rhodium bond.[8b,23]

A κ^3-*P,P,M* ligand coordination in **7**, **8**, and **10** was readily inferred by a significant decrease of the value of the Rh−P coupling constant (ca. 90 Hz) as well as by ^1H NMR $\Delta\delta$ values, relative to the α and β hydrogen atoms of the Cp rings, of ca. 1.2 ppm. Indeed, in a trigonal-bipyramidal structure with *trans* P atoms, the larger dihedral angle between the two Cp planes increases the difference of the chemical shift of the α and β hydrogen atoms of the Cp rings.[8a,c,23] Since the trigonal-bipyramidal complexes **7**, **8**, and **10** are stereochemically rigid in solution, the observed ν(CO) bands (2020−2040 and 1990−1980 cm^{-1}) may be safely assigned to equatorial *cis* CO ligands.[24]

The formation of κ^3-*P,P,M* 1,1′-bis(diarylphosphino)-metallocene complexes, as in **7**, **8**, and **10**, is controlled by both steric and electronic factors.[8a,c,23] In particular, the κ^3-*P,P,M* bonding mode is promoted by the presence of alkyl substituents on either Cp or P-aryl groups, while the strength of the metal−metal dative bond increases in the order Fe < Ru < Os, due to the increasing diffusion of the metal-centered e_{2g} electron density down to the iron triad.[23a−c]

A square-planar geometry for **6** and a trigonal-bipyramidal geometry for **8** were unequivocally confirmed also in the solid state by single-crystal X-ray analyses. ORTEP plots of the complex cations $[Rh(CO)_2(dppf)]^+$ and $[Rh(CO)_2(dppo)]^+$ are reported in Figure 1. Crystallographic data for both compounds and selected bond lengths and angles are reported in Table 1 and Table 2, respectively.

In **6**, the rhodium center is square-planarly coordinated by a chelating dppf ligand and by two terminal carbonyl groups. Deviations from the ideal geometry are put in evidence by the *trans* angles P(1)−Rh(1)−C(2) and P(2)−Rh(1)−C(1) of 175.5(2)° and 171.7(2)°, respectively, with the rhodium atom displaced by 0.049 Å from the least-squares plane passing through the P and the C_{CO} donors. The ferrocenyl moiety, with the Fe−$Cp_{centroid}$ distances averaging 1.642(3) Å and the $Cp_{1centroid}$−Fe(1)−$Cp_{2centroid}$ of 179.1(2)°, adopts an ar-

Table 2. Selected Bond Lengths [Å] and Angles [deg] for 6 and 8[a]

	6	**8**
Rh(1)−P(1)	2.357(1)	2.286(6)
Rh(1)−P(2)	2.371(1)	2.283(6)
Rh(1)−C(1)	1.888(5)	1.74(3)
Rh(1)−C(2)	1.893(5)	1.81(4)
Fe(1)−C_{Cp1} (av)	2.035(12)	
Fe(1)−$Cp_{1centroid}$	1.639(5)	
Fe(1)−C_{Cp2} (av)	2.038(7)	
Fe(1)−$Cp_{2centroid}$	1.644(5)	
Os(1)−C_{Cp1} (av)		2.20(2)
Os(1)−$Cp_{1centroid}$		1.82(2)
Os(1)−C_{Cp2} (av)		2.19(2)
Os(1)−$Cp_{2centroid}$		1.84(2)
O(1)−C(1)	1.123(6)	1.20(3)
O(2)−C(2)	1.134(6)	1.16(3)
Rh(1)···Fe(1)	4.234(1)	
Rh(1)···Os(1)		3.139(2)
P(1)−Rh(1)−P(2)	95.96(4)	155.9(2)
C(1)−Rh(1)−C(2)	87.4(2)	123.8(18)
C(1)−Rh(1)−P(1)	88.53(15)	94.9(8)
C(2)−Rh(1)−P(1)	175.49(15)	92.4(11)
C(1)−Rh(1)−P(2)	171.7(2)	97.8(9)
C(2)−Rh(1)−P(2)	88.30(15)	97.4(10)
$Cp_{1centroid}$−Fe(1)−$Cp_{2centroid}$	179.1(2)	
$Cp_{1centroid}$−Os(1)−$Cp_{2centroid}$		165.9(9)
O(1)−C(1)−Rh(1)	175.3(6)	167(3)
O(2)−C(2)−Rh(1)	176.8(4)	179(3)

[a] Cp_1: C(51)−C(55); Cp_2: C(61)−C(65).

(22) (a) Betley, Th. A.; Peters, J. C. *Angew. Chem., Int. Ed*. **2003**, *42*, 2385. (b) Fairle, D. P.; Bosnich, B. *Organometallics* **1988**, *7*, 946.
(23) (a) Sato, M.; Shigeta, H.; Sekino, M.; Akabori, S. *J. Organomet. Chem*. **1993**, *458*, 199. (b) Zuideveld, M. A.; Swennenhuis, B. H. G.; Boele, M. D. K.; Guari, Y.; van Strijdonck, G. P. F.; Reek, J. N. H.; Kamer, P. C. J.; Goubitz, K.; Fraanje, J.; Lutz, M.; Spek, A. L.; van Leeuwen, P. W. N. M. *J. Chem. Soc., Dalton Trans*. **2002**, 2308. (c) Zuideveld, M. A.; Swennenhuis, B. H. G.; Kamer, P. C. J.; van Leeuwen, P. W. N. M. *J. Organomet. Chem*. **2001**, *637*, 805. (d) Akabori, S.; Kumagai, T.; Shirahige, T.; Sato, S.; Kawazoe, K.; Tamura, C.; Sato, M. *Organometallics* **1987**, *6*, 526. (e) Akabori, S.; Kumagai, T.; Shirahige, T.; Sato, S.; Kawazoe, K.; Tamura, C.; Sato, M. *Organometallics* **1987**, *6*, 2105.
(24) (a) Dixon, F. M.; Eisenberg, A. H.; Farrell, J. R.; Mirkin, C. A.; Liable-Sands, L. M.; Rheingold, A. L. *Inorg. Chem*. **2000**, *39*, 3432. (b) Siegl, W. O.; Lapporte, S. J.; Collman, J. P. *Inorg. Chem*. **1971**, *10*, 2158.

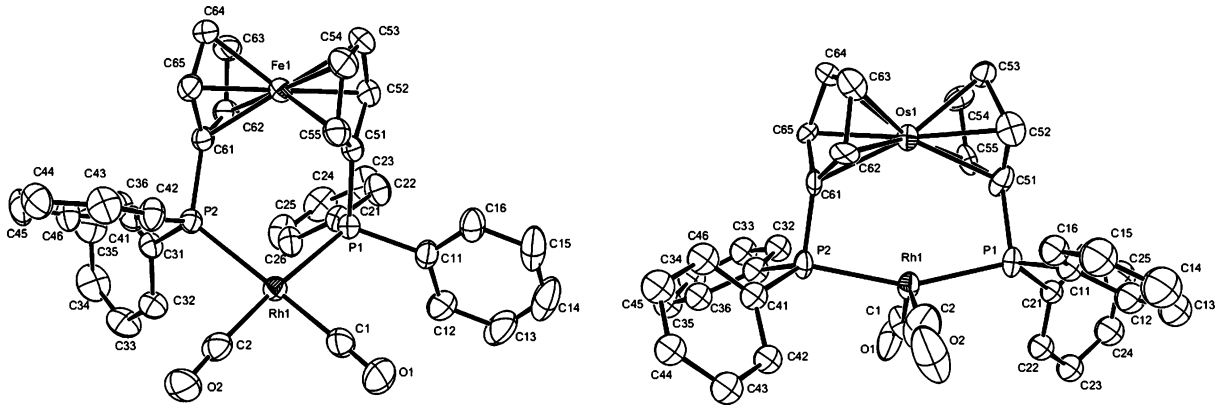

Figure 1. ORTEP plots of **6** (left) and **8** (right). Thermal ellipsoids are shown at the 30% probability level. The PF_6 anions have been omitted for clarity.

Table 3. Hydroformylation of 1-Hexene Using [Rh(P−P)(COD)]X Complexes[a] (P−P: 1,1′-bis(diarylphosphino)metallocene)

run	precatalyst/ ligand	time (h)	conversion (%)	TOF[b]	hydroformylation products (%)	selectivity[c] (%)	hexane (%)	1-heptanol (%)	isomerization (%)
1	**1a**/dppf	1	68.3	683	52.1	67.1	0	0	16.2
2	**1a**/dppf	2	75.1	376	59.5	73.5	0.6	0	15.0
3	**2**/dppr	1	65.2	652	49.1	69.7	0.1	0	16.0
4	**2**/dppr	2	93.2	466	71.7	72.0	0.8	0	20.7
5	**3a**/dppo	1	32.8	328	20.7	69.4	3.3	0	8.9
6	**3a**/dppo	2	98.9	495	68.4	72.3	3.7	1.1	25.6
7	**4**/dppomf	1	98.8	988	67.1	63.5	0.8	2.5	28.4
8	$[RhCl(COD)]_2$	1	98.9	988	63.4	62.8	0.9	4.3	30.2
9	**5**/*o*-^{i}Pr-dppf	1	71.9	719	52.9	67.2	0	0	18.9
10	**5**/*o*-^{i}Pr-dppf	2	76.4	382	56.4	72.5	0.7	1.7	17.6

[a] Reaction conditions: precatalyst 2 μmol; substrate 2 mmol; 25 mL THF; 45 bar CO/H_2 (1:2) at 20 °C; reaction temperature 60 °C; stirring rate 300 rpm. [b] Expressed as (mol of aldehyde) (mol of Rh)$^{-1}$ h^{-1}. [c] Selectivity towards the linear aldehyde.

rangement of minimum repulsion with respect to the phenyl rings. Consistently, the Cp groups exhibit a staggered conformation, with the torsion angle P(1)−$Cp_{1centroid}$−$Cp_{2centroid}$−P(2) of 32.7°. The rhodium−iron distance of 4.234 Å excludes any interaction between the two metals, the sum of the covalent radii of Rh and Fe being 2.69 Å.

The larger atom radius of osmium as compared to iron (1.35 vs 1.26 Å) and the larger distances of the Cp rings from the Os center (1.83(2) Å) well account for the short Rh−Os distance (3.139(2) Å) observed in the structure of **8**, which indicates the occurrence of a weak, yet actual, metal−metal bonding interaction.[25] The two Cp rings in **8** are not parallel to each other, which is shown by the $Cp_{1centroid}$−Os(1)−$Cp_{2centroid}$ angle of 165.9(8)°. Indeed, the two Cp rings deviate from an eclipsed conformation by an angle of 27.3°. The carbonyl groups dispose themselves in the equatorial plane of a distorted trigonal-bipyramid, and P(1) and P(2) occupy the pseudo-axial position with an P(1)−Rh(1)−P(2) angle of 155.9-(2)°. A similar *cis* disposition of the CO ligands has been observed by Erker in a 1,1′-bis(diphenylphosphino)-(methyl)zirconocene dicarbonyl rhodium complex.[26] This exhibits a very distorted trigonal-bipyramidal structure with a Zr−Rh bond length of 2.444(1) Å and a CO−Rh−CO angle of 107.8°. The values of the Rh−P distances averaging 2.364(7) and 2.284(2) Å respectively in **6** and **8** are in agreement with the *trans* influence exerted by the opposite CO groups. The CO groups in **6** exhibit comparable linearity and substantially equal Rh−C (1.89 Å av) and C−O (1.14 Å av) bond distances.[22a] The two carbonyl groups in **8** are less defined, due to the poor quality of the data, and therefore a truly reliable comparison with compound **6** cannot be made.

Batch Hydroformylation Reactions. The performance of **1a**, **2**, **3a**, **4**, and **5** as catalyst precursors for the hydroformylation of 1-hexene was investigated in THF in a standard, mechanically stirred autoclave. Following a partial optimization procedure, these conditions were selected to compare the activity and regioselectivity of the catalysts investigated: substrate-to-catalyst ratio 1000, 60 °C, 45 bar CO/H_2 (1:2). The results are reported in Table 3.

From a perusal of the data reported in Table 3, one may readily infer that the dppf, dppr, and dppo precursors display a similar catalytic behavior, especially in terms of regio- and chemoselectivity. The only noticeable difference is provided by the conversions at 1 and 2 h: a longer induction period seems to affect the dppo catalyst, as it is much less productive than the dppf one within 1 h, but it gives almost complete conversion of the substrate after 2 h (runs 1/2 vs 5/6). The dppr catalyst **2** lies midway between the dppf and dppo ones (runs 3/4).

At first glance, the dppomf catalyst appears as the most active with an almost complete transformation of

(25) (a) Trepanier, S. J.; McDonald, R.; Cowie, M. *Organometallics* **2003**, *22*, 2638. (b) Trepanier, S. J.; Sterenberg, B. T.; McDonald, R.; Cowie, M. *J. Am. Chem. Soc*. **1999**, *121*, 2613. (c) Sterenberg, B. T.; McDonald, R.; Cowie, M. *Organometallics* **1997**, *16*, 2297. (d) Sterenberg, B. T.; Hilts, R. W.; Moro, G.; McDonald, R.; Cowie, M. *J. Am. Chem. Soc*. **1995**, *117*, 245. (e) Hilts, R. W.; Franchuk, R. A.; Cowie, M. *Organometallics* **1991**, *10*, 304.

(26) (a) Cornelissen, C.; Erker, G.; Kehr, G.; Fröhlich, R. *Organometallics* **2005**, *24*, 214. (b) Cornelissen, C.; Erker, G.; Kehr, G.; Fröhlich, R. *Dalton Trans*. **2004**, 4059.

1-hexene in 1 h and a selectivity in aldehydes of 67% (run 7). However, a perusal of the product distribution and a comparison with the results obtained with the unmodified catalyst precursor $[RhCl(COD)]_2$ (run 8) raised a doubt about the true nature of the catalyst generated by **4**. This doubt became a certainty after the reaction was studied by HP-NMR and HP-IR under hydroformylation conditions that clearly showed a significant degradation of **4** to various compounds, including phosphine-free rhodium carbonyls (see below).

The slight increase in 1-hexene conversion exhibited by the *o*-^{i}Pr-dppf catalyst **5** in the second hour (see runs 9 and 10) was initially taken as an indication of effective catalyst degradation within the first 60 min. On the other hand, the enhanced production of linear aldehyde in the second hour was still consistent with a phosphine-modified catalyst. A clue to rationalize the behavior of **5** was later provided by *operando* HP-NMR and HP-IR experiments that showed **5** to be unable to generate a hydride(dicarbonyl) resting state (see below), which may indicate a different hydroformylation mechanism as compared to **1a**, **2**, and **3a**.

Finally, all the catalysts promote significant isomerization of 1-hexene, which is consistent with the experimental conditions.

***Operando* NMR and IR Studies.** The hydroformylation of 1-hexene assisted by **1a**, **2**, **3b**, **4**, and **5** was investigated by HP-NMR and HP-IR spectroscopy under experimental conditions comparable to those used in the batch reactions. An almost perfect coincidence of experimental conditions could be adopted only for the HP-IR experiments, as the IR cell was a real autoclave. In contrast, the HP-NMR experiments were carried out in 10 mm-o.d. sapphire tubes that, although spinning regularly, cannot prevent the occurrence of mass-transfer limitation due to the lack of effective stirring. Moreover, a higher concentration of catalyst precursors was actually used in the HP-NMR experiments to have a better signal-to-noise ratio. On the other hand, the combination of HP-IR and HP-NMR experiments allowed us to look at catalytic reactions on different time scales as well as take advantage of the inherent mass-transfer limitation of the HP-NMR technique to intercept kinetic products.

Typically, THF-d_8 solutions of **1b**, **2**, **3b**, **4**, and **5** were pressurized in a 10 mL sapphire tube with CO/H_2 (1:2) to a total pressure of 45 bar at room temperature. After acquiring $^{31}P\{^1H\}$ and ^1H NMR spectra, the solutions were gradually heated to 60 °C. For every thermal step (ca. 10 °C), a residence time of 10 min was chosen before acquiring the next NMR spectrum. Irrespective of the rhodium precursor, either square-planar or trigonal-bipyramidal dicarbonyl Rh^I complexes were formed at room temperature and COD was released in solution. A slight anomalous behavior was exhibited by the dppf complex. For this reason a sequence of $^{31}P\{^1H\}$ NMR spectra relative to the reaction catalyzed by **1b** is shown in Figure 2, while Scheme 2 illustrates the results for all the complexes investigated.

The dppf precursor completely converted to two species already at room temperature: the square-planar dicarbonyl **6** and another compound, hereafter quoted as **15** (Figure 2b). Complex **15** is featured by a $^{31}P\{^1H\}$ doublet at 24.92 ppm with $J(PRh) = 91.6$ Hz and ^1H NMR data for the α and β hydrogen atoms of the Cp's that are indicative of a *transoid* disposition of the P donor atoms ($\Delta\delta = 0.85$ ppm).[8c,23]

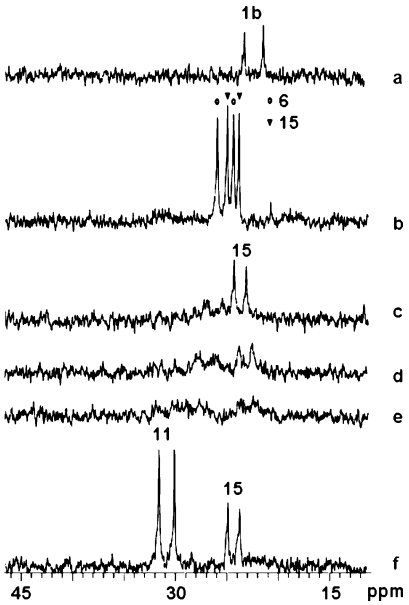

Figure 2. $^{31}P\{^1H\}$ NMR spectra acquired in the course of the hydroformylation of 1-hexene in THF-d_8 catalyzed by **1b**: (a) **1b** in the presence of 1-hexene at room temperature under nitrogen; (b) after the tube was pressurized with CO/H_2 (1:2) to a total pressure of 45 bar at room temperature; (c) 40 °C, (d) 50 °C, (e) 60 °C; (f) after the tube was cooled to room temperature.

Scheme 2

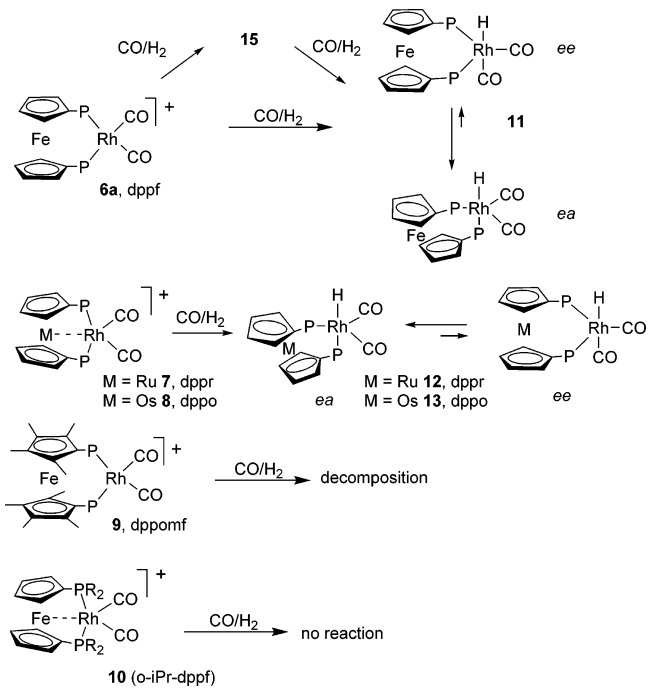

As the temperature was increased to 40 °C, **6** rapidly disappeared while the other signal broadened (Figure 2c). Further increasing the temperature to 50 °C and then to 60 °C caused both resonances to disappear with a concomitant increase of the noise-to-signal ratio, which is typical of NMR spectra taken during a catalytic reaction where multiple equilibra are at work (Figure 2d,e).[16,27]

When the temperature of the probe-head was cooled to room temperature, two well-resolved resonances reappeared in the spectrum: one was due to **15**, the other to a new species that was safely identified as the known trigonal-bipramidal hydride(dicarbonyl) Rh^I complex $RhH(CO)_2$(dppf) (**11**) (Figure 2f).[11] The formation of the latter complex apparently requires that H_2 is heterolytically split at rhodium, a process that has several precedents, especially for hydrogenation reactions carried out in a nucleophilic solvent such as THF.[28] As a matter of fact, **11** was not obtained by treatment of **1b** with syngas in a nonbasic solvent such as CH_2Cl_2. The identification of **11** was straightforward on the basis of previous studies by van Leeuwen and coworkers.[11] The NMR parameters ($^{31}P\{^1H\}$ doublet and ^1H triplet of doublets for the terminal hydride ligand) observed for **11** are averaged values due to a fast interconversion between equatorial−equatorial (ee) and equatorial−axial (ea) geometric isomers (Scheme 2), likely proceeding via turnstyle or Berry-type (pseudo)-rotation.[29] Interestingly, the two isomers, which interconvert into each other faster than the NMR time scale, could be distinguished by HP-IR spectroscopy (see below). At this point it may be worthwhile to recall that the hydride(dicarbonyl) compounds are commonly regarded as true precatalysts for the hydroformylation of alkenes by rhodium complexes with chelating diphosphines. From hydride(dicarbonyl) compounds, CO decoordination occurs, followed by alkene complexation, to regenerate five-coordinate intermediates.[30]

All our attempts to unambiguously characterize **15** were unsuccessful. This compound is actually unstable: it slowly converted to **11** in the NMR tube even at room temperature and disappeared completely by venting the NMR tube with N_2. A number of independent experiments were carried out in an attempt to identify **15**: (i) Isolated **6** was dissolved in THF-d_8 and the solution was introduced into a HP-NMR tube. Upon pressurization with CO (up to 30 bar), no other compound than **6** was seen by NMR spectroscopy from room temperature to 60 °C. Only when the tube was pressurized with 45 bar CO/H_2 (1:2) did **6** start to convert into **15**. (ii) The same experiment as in (i) was performed in CD_2Cl_2. No conversion into **15** was observed even in the presence of syngas, irrespective of the pressure and temperature. (iii) When the hydroformylation of 1-hexene catalyzed by **1b** was studied by *operando* HP-IR spectroscopy under fast and effective mixing of the reactants (see below), no trace of **15** was detected. (iv) Isolated **6** was dissolved in THF-d_8 and the solution was introduced into an HP-NMR tube. Upon pressurization with H_2 (up to 30 bar) at room temperature, some hydride(dicarbonyl) **11** was formed, but together with several unknown, probably reduced, species.

Chart 3

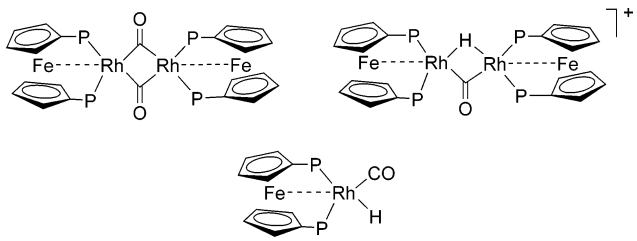

Incorporation of all of these results with the NMR data for **15** led us to conclude that (i) the P atoms in **15** are likely *transoid* to each other. (ii) **15** requires the concomitant presence of H_2 and CO to form, yet these two reagents must be in low concentration as occurs in the mass-transfer limitation conditions of the HP-NMR experiment. Indeed, under vigorous stirring as occurs in the HP-IR cell, neither **6** nor **15** was seen and **1b** was straightforwardly converted into **11** even at room temperature (see below). (iii) The formation of **15** requires a basic solvent to be accomplished. A number of possible structures for dppf metal complexes are fully or partially consistent with the experimental observables listed above (Chart 3), yet none of them have been unequivocally proved.

A much simpler HP-$^{31}P\{^1H\}$ NMR picture was observed for the dppr and dppo catalysts under hydroformylation conditions. In either case, the dicarbonyl intermediates were initially formed and the neutral hydride(dicarbonyl) compounds were the only detectable Rh compounds present in the reaction mixtures in the course (see HP-IR study below) and at the end of the hydroformylation catalysis (Scheme 2). The conversion of the dppo derivative **8** into $RhH(CO)_2$(dppo) (**13**) was significantly slower (3 h at 60 °C) than that of the dppr analogue $RhH(CO)_2$(dppr) (**12**) (<1 h). Again, averaged values for H−P and Rh−P coupling constants were observed in the NMR spectra.

In contrast to **1b**, **2**, and **3b**, neither **4** nor **5** generated hydride(dicarbonyl) compounds when reacted with syngas in the HP-NMR tube with or without added 1-hexene. The dppomf derivative, after forming a square-planar dicarbonyl at room temperature, underwent extensive decomposition to binary CO rhodium compounds as the temperature was increased to 60 °C (see HP-IR experiment below), while the *o*-^{i}Pr-dppf dicarbonyl complex **10** remained unchanged even after 2 h at 60 °C. In separate experiments, the dicarbonyl complexes **9** and **10** were reacted with syngas in the presence of NEt_3, which is known to promote the heterolytic splitting of H_2.[28] Under these conditions, the hydride(dicarbonyl) $RhH(CO)_2$(dppomf) (**14**) was selectively obtained even at room temperature, while **10** decomposed to give rhodium−carbonyl compounds and free metallocenylphosphine ligand.

Parallel to the HP-NMR investigation, an HP-IR study of the hydroformylation reactions catalyzed by **1b**, **2**, **3b**, **4**, and **5** was carried out under conditions comparable to those of the batch reactions, except for a substrate-to-catalyst ratio of 100. IR traces in the CO stretching region, recorded at 60 °C, are reported in Figure 3 for all reactions.

(27) Bianchini, C.; Lee, H. M.; Barbaro, P.; Meli, A.; Monetti, S.; Vizza, F. *New J. Chem*. **1999**, *23*, 929.
(28) Bianchini, C.; Moneti, S.; Peruzzini, M.; Vizza, F. *Inorg. Chem.* **1997**, *36*, 5818.
(29) (a) Berry, R. S. *J. Chem. Phys*. **1960**, *32*, 933. (b) Meakin, P.; Muetterties, E. L.; Jesson, J. P. *J. Am. Chem. Soc*. **1972**, *94*, 5271. (c) Buisman, G. J. H.; van der Veen, L. A.; Kamer, P. C. J.; van Leeuwen, P. W. N. M. *Organometallics* **1997**, *16*, 5681. (d) Casey, C. P.; Paulsen, E. L. Beuttenmueller, E. W.; Proft, B. R.; Matter, B. A.; Powell, D. R. *J. Am. Chem. Soc*. **1999**, *121*, 63. (e) Castellanos-Páez, A.; Castillon, S.; Claver, C.; van Leeuwen, P. W. N. M.; de Lange, W. G. J. *Organometallics* **1998**, *17*, 2543.
(30) (a) Van Leeuwen, P. W. N. M.; Kamer, P. C. J.; Reek, J. N. H.; Dierkes, P. *Chem. Rev*. **2000**, *100*, 2741. (b) Van der Veen, L. A.; Keeven, P. H.; Schoemaker, G. C.; Reek, J. N. H.; Kamer, P. C. J.; van Leeuwen, P. W. N. M.; Lutz, M.; Spek, A. L. *Organometallics* **2000**, *19*, 872. (c) Casey, C. P.; Whiteker, G. T.; Melville, M. G.; Petrovich, L. M.; Gavney, J. A.; Powell, D. R. *J. Am. Chem. Soc*. **1992**, *114*, 5535.

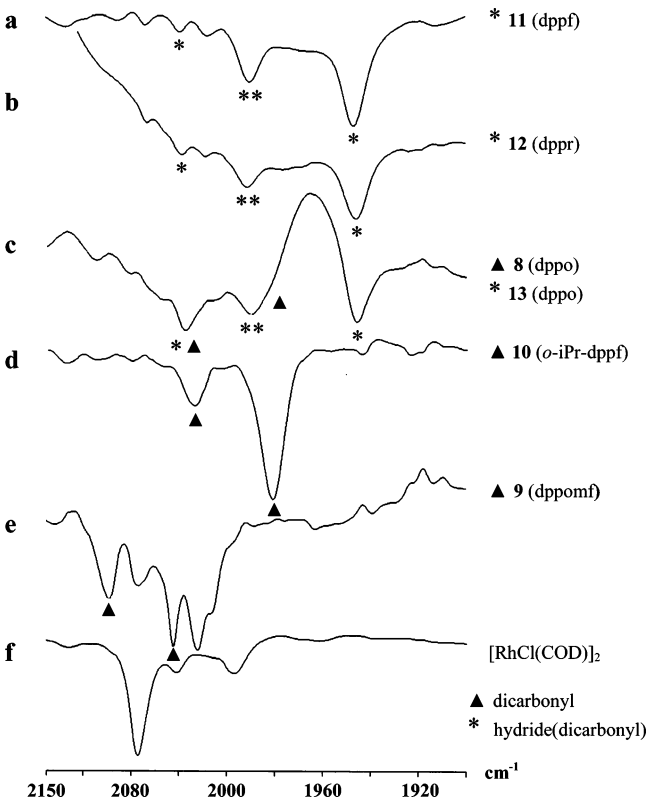

Figure 3. HP-IR spectra acquired after 1 h of the hydroformylation of 1-hexene catalyzed by [Rh(P−P)(COD)]X (THF, 60 °C, 45 bar 1:2 CO/H_2).

Irrespective of the temperature, pressurization of the autoclave with 45 bar syngas caused the COD precursors **1b** and **2** to transform rapidly and selectively into the hydride(dicarbonyl) compounds **11** and **12**, respectively (Figure 3a,b). In agreement with the NMR study, the dppo precursor **3b** converted to the hydride(dicarbonyl) **13** more slowly than the dppf and dppr precursors (Figure 3c). Indeed, the complete transformation required 2 h at 60 °C. No trace of hydride(dicarbonyl) complex was observed starting from the *o*-^{i}Pr-dppf precursor, whose dicarbonyl product **10** was stable for 2 h at 60 °C (Figure 3d). A dicarbonyl product was also obtained with the dppomf precursor; however soon after its formation, the dicarbonyl **9** started decomposing to give, inter alia, phosphine-free rhodium compounds (Figure 3e) that were also obtained by the reaction of $[RhCl(COD)]_2$ with syngas (Figure 3f).[31]

Besides confirming the transient nature of the dicarbonyl complexes and the resting-state nature of the hydride(dicarbonyl) complexes with dppf, dppr, and dppo, the HP-IR experiments provided further valuable information: (i) The dppomf dicarbonyl intermediate undergoes decomposition to several CO rhodium species, which include compounds with no coordinated phosphine. (ii) The dynamic equilibrium that averages the NMR parameters of the ee and ea stereoisomers of the hydride(dicarbonyl) complexes **11**, **12**, **13**, and **14** (this compound was independently prepared by adding NEt_3, vide infra) is slow on the IR time scale. Accordingly, both conformers were detected and the intensity ratio of the relative ν(CO) bands showed that the metallocenyldiphosphines investigated prefer to bind rhodium in ea fashion, which accounts for the regioselectivity observed in the batch reactions (67−74% in linear aldehyde).[11,30b,32]

Conclusions

The hydroformylation of 1-hexene catalyzed by 1,1′-bis(diarylphosphino)metallocene rhodium(I) complexes has been investigated, for the first time, by both HP-NMR and HP-IR spectroscopy under catalytic conditions. In the absence of this study, the hydroformylation results, especially as regards the chemo- and regioselectivity (Table 3), would have misled one to conclude that all diphosphine rhodium precursors generate similar catalytic systems, where unmodified catalysts, formed upon degradation of the modified catalysts, contribute to the overall catalytic outcome. Just the *operando* studies have made clear that this is not true, unambiguously showing that both the mechanism and the catalytic activity are actually controlled by the structure of the diphosphine ligand. On the other hand, it is also apparent that the structural variations of the 1,1′-bis(diarylphosphino)metallocenes investigated in this study affect significantly neither the chemoselectivity nor the regioselectivity.

The main conclusions provided by the present study may be summarized as follows.

Irrespective of the catalyst precursor, all the steps involved in the hydroformylation reaction at 60 °C are faster than the NMR time scale, including the generation of the catalyst from the hydride(dicarbonyl) resting state. Noteworthy, the latter process seems to be rate limiting, as the hydride(dicarbonyl) compounds are the only species visible on the IR time scale during the catalytic reactions.

The activation of H_2 in THF is heterolytic in nature for the dppf, dppr, dppo, and dppomf precursors. Moreover, the activity of the 1,1′-bis(diarylphosphino)metallocene rhodium(I) catalysts is significantly influenced by the formation (and strength) of dative metal−rhodium bonds in the Rh^I dicarbonyl intermediates which are precursors to the Rh^I hydride(dicarbonyl) resting states. The low productivity of the dppo precursor in the first hour is therefore attributable to the remarkable strength of the dative Os−Rh bonding interaction in the corresponding dicarbonyl complex. However, the dppo catalyst is also more efficient than the dppf and dppr catalysts in the second hour, which suggests that a strong intramolecular Os−Rh bond may be important in stabilizing other five-coordinate catalytic intermediates toward their degradation to phosphine-free species. Severe degradation has been proved for the catalyst with dppomf, which, in fact, does not form a dative Fe−Rh bond.

Another case is represented by the *o*-^{i}Pr-dppf ligand: it promotes the formation of a κ^3-*P,P,M* dicarbonyl complex, but not of a hydride(dicarbonyl) compound even in THF. The failure of the *o*-^{i}Pr-dppf dicarbonyl complex to activate H_2 in a heterolytic fashion may be due to the four bulky *o*-^{i}Pr groups. These may either

(31) (a) Buisman, G. J. H.; Vos, E. J.; Kamer, P. C. J.; van Leeuwen, P. W. N. M. *J. Chem. Soc., Dalton Trans*. **1995**, 409. (b) Garland, M.; Pino, P. *Organometallics* **1991**, *10*, 1693.

(32) Van der Veen, L. A.; Boele, M. D. K.; Bregman, F. R.; Kamer, P. C. J.; van Leeuwen, P. W. N. M.; Goubitz, K.; Fraanje, J.; Schenk, H.; Bo, C. *J. Am. Chem. Soc.* **1998**, *120*, 11616.

reinforce the dative Fe−Rh bond by favoring a *trans* arrangement of the P atoms[8a,b,23] or disfavor the external nucleophilic attack by THF or NEt_3, which is required for the heterolytic splitting of activated H_2.[28]

Acknowledgment. This work has been supported by the CNR Department "Molecular Design" within the project "Design of molecules and nanostructures with catalytic properties". Thanks are also due to Mr. Aldo Traversi and Carlo Bartoli for the construction of the high-pressure NMR and IR instruments.

Supporting Information Available: Crystallographic tables and tables of atomic coordinates, bond distances and angles, anisotropic thermal parameters, and hydrogen coordinates for compounds **6** and **8** are available free of charge via the Internet at http://pubs.acs.org.

OM050241L